International Soil and Water Conservation Research 13 (2025) 1–14

Contents lists available at ScienceDirect

International Soil and Water Conservation Research

journal homepage: www.elsevier.com/locate/iswcr

Original Research Article

Effects of initial soil moisture on rill erodibility and critical shear stress factors in the WEPP model across diverse soil types

Fikret Ari [a], Selen Deviren Saygin [b, *], Cagla Temiz [b], Sefika Arslan [b], Mehmet Altay Unal [c], Gunay Erpul [b], Dennis C. Flanagan [d]

[a] Department of Electrical and Electronics Engineering, Faculty of Engineering, Ankara University, 06830, Golbasi, Ankara, Turkey
[b] Department of Soil Science and Plant Nutrition, Faculty of Agriculture, Ankara University, 06110, Diskapi, Ankara, Turkey
[c] Stem Cell Institute, Ankara University, 06520, Cankaya, Ankara, Turkey
[d] USDA-Agricultural Research Service, National Soil Erosion Research Laboratory, 275 S. Russell St., West Lafayette, IN, 47907-2077, USA

ARTICLE INFO

Article history:
Received 11 May 2024
Received in revised form
12 September 2024
Accepted 3 October 2024
Available online 6 October 2024

Keywords:
Soil erosion by water
Rill erosion
Erodibility parameters
Soil hydrology
Soil cohesion

ABSTRACT

Rill erosion, a significant issue in agricultural regions, is intricately linked to initial soil moisture conditions, affecting the development of concentrated flow erosion processes. However, understanding its dynamics amidst varying soil moisture conditions remain challenging. This study aimed to assess the impact of different soil moisture levels on rill erodibility parameters in the Water Erosion Prediction Project (WEPP) model and to evaluate soil cohesion across a spectrum of soils. Through laboratory experiments employing a small V-shaped rill channel, we investigated rill erodibility (K_r) and critical hydraulic shear stress (τ_{cr}), under three soil moisture scenarios: initially dry, saturated, and drainage, with incremental surface inflow rates. Additionally, we examined the efficiency of soil cohesion obtained from an Automated Soil Cohesion Measurement Apparatus in predicting K_r and τ_{cr} across various soil textures. Our analysis encompassed twenty soils representing nine texture classes, revealing significant correlations between basic soil properties, cohesion parameters, and WEPP model rill erodibility. Notably, initial soil moisture conditions exerted substantial influence on erodibility potentials. Soils with higher silt contents demonstrated better fits in terms of Nash-Sutcliffe model efficiency, particularly under initially dry and saturated conditions. However, predictions for initially drained soils yielded poor fits, emphasizing the intricate interplay between soil properties and hydrological conditions. In conclusion, our findings emphasize the critical role of topsoil water dynamics in rill erodibility. We propose that soil cohesion serves as a valuable predictor, complementing friction forces within the soil and enhancing simulations of rill erodibility under shallow flow conditions in rills, particularly in next-generation process-based modeling approaches.

1. Introduction

Erosion is primarily responsible for land degradation in cultivated areas located in fragile ecosystems, and is a significant threat to sustainability ([FAO & ITPS, 2015). Water erosion, which is the most widespread type of soil erosion is one of the most important problems encountered in arid and semi-arid countries to ensure sustainable agricultural systems and achieve the goals of safe food and environmental protection, along with the negative effects of climate change. The “Turkey Water Erosion Atlas” stated that 642 million tonnes of soil are eroded every year in Turkey. Of this total, 154 million tonnes are carried away by streams and away from the soil system corresponding to an approximately 2 tonnes per hectare of fertile topsoil layer lost (Erpul et al., 2018).

Erodibility is the susceptibility of a soil to detachment by erosive agents (e.g., flowing water), and mostly correlates with intrinsic soil properties, and is an important input to erosion prediction models. In general, the erodibility potential of soils tends to decline as

* Corresponding author.
E-mail addresses: fari@eng.ankara.edu.tr (F. Ari), sdeviren@agri.ankara.edu.tr (S.D. Saygin), almond_cagla89@hotmail.com.tr (C. Temiz), sefikaarslan77@gmail.com (S. Arslan), altay.unal@ankara.edu.tr (M.A. Unal), erpul@ankara.edu.tr (G. Erpul), dennis.flanagan@usda.gov (D.C. Flanagan).

https://doi.org/10.1016/j.iswcr.2024.10.001

organic matter, clay content, stoniness and soil aggregate median diameter increase (Alberts et al., 1995; Chenu et al., 2000; Panagos et al., 2014; Potter et al., 2002; Rapp, 2000; Reichert et al., 2009; Sheridan et al., 2000; Yu et al., 2014). The soil erodibility varies through time due to its close relationships with other factors e.g. vegetative, climatic, and hydrologic conditions (Bryan, 2000; Deviren Saygın, 2021).

The initial soil moisture content is a significant feature by driving the soil detachment and sediment transport processes and resulting soil losses (Liu et al., 2017). Particularly in rill erosion, which is one of the most significant water erosion types in agricultural areas, initial moisture content can affect internal soil strength (Deviren Saygin et al., 2018; Huang et al., 1996; Mamedov et al., 2006; Römkens et al., 2002; Shainberg et al., 2003; Zheng et al., 2020) and subsequent rill development. However, soil moisture has multifaceted effects on rill erodibility. Current studies have shown that an increase in soil moisture can lead to an increase in rill erodibility due to a decrease in soil cohesion (Knapen et al., 2007; Nachtergaele & Poesen, 2002; Poesen, 2007; Van Klaveren & McCool, 1998; Wang et al., 2020; Wang, Flanagan, & Engel, 2021; Wang, Flanagan, Engel, et al., 2021; Yu et al., 2014). However, stronger cohesion development and lower erodibility can be observed under seepage conditions where the soil has higher moisture content (Grissinger, 1966, 1972; Hanson et al., 1999; Knapen et al., 2007). When initial soil moisture content is low, rill erodibility can be high since soil particles are not free to reorient themselves to a position with low energy and high cohesion between particles (Knapen et al., 2007; Shainberg et al., 1996). This situation is closely related to the initial strength of soil under flow conditions and the drivers of aggregate formation mechanisms e.g., primary soil particles, bonding agents, etc. (Amezketa, 1999; Deviren Saygin et al., 2018; Shainberg et al., 1996).

The USDA Water Erosion Prediction Project (WEPP) model is a process-based, computer simulation program that simulates many physical processes (e.g., infiltration, runoff, plant growth, sediment detachment, transport, and deposition). WEPP erosion prediction technology estimates daily, monthly, annual, or average annual values of runoff and soil erosion (Deviren Saygin et al., 2018; Flanagan et al., 2007; Flanagan & Nearing, 1995; Nearing et al., 1990).

Baseline soil erodibility parameters for prediction of rill and interrill detachment in the WEPP model can be estimated using three different sets of independent equations (Alberts et al., 1995; Flanagan & Livingston, 1995). The three erodibility parameters are interrill erodibility (K_i), rill erodibility (K_r), and critical shear stress (τ_{cr}) (Flanagan et al., 2001), but direct measurement of K_i, K_r and τ_{cr} under field conditions is difficult, costly and time-consuming. For overcoming this challenge, Shainberg et al. (1994) proposed a methodology to evaluate K_r and τ_{cr} values in laboratory conditions with a mini-flume which was 0.5 m long, 0.046 m wide, and 0.12 m deep. Two V-shaped channels, 0.2 m long, were cemented to the flumes, one at each side. Water flow in the entry channel minimized turbulence and any pulse flow. The channels at both ends helped to minimize any edge effects. They stated that K_r values measured in the laboratory study were similar to those determined for the same soil in a field study, but their results were opposite for the critical shear stress values. τ_{cr} values were considerably lower in the laboratory study due to differences in soil structure and experimental procedures.

Likewise, Wu et al. (2017) and Deviren Saygin et al. (2018) used these mini-flumes to experimentally measure K_r and τ_{cr} values in the WEPP model for medium to coarse textured soil types under three different moisture contents: initially dry, saturated, and drainage. Results revealed that hydrologic conditions could be a significant factor by driving the soil detachment and sediment transport processes and resulting soil loss rates, and the effects of initial soil moisture conditions on rill initiation need to be taken into consideration in erosion models. Although the behavior of soil as a cohesive material in water is extremely important for predicting sedimentation and disintegration, studies on the subject indicate that the roles of these physicochemical forces affecting soil cohesion on erodibility, disintegration and transport mechanisms are not yet fully understood (Simon & Collison, 2001; Wang et al., 2019). Other studies have also drawn attention to the effects of increasing water pressure on rill development and fragmentation processes on shallow overland flow supported sediment concentrations (Huang et al., 1996; Nearing et al., 1997; Römkens et al., 2002; Wang et al., 2020; Zhang et al., 2019). These studies have shown that experimentally determined erodibility parameters are affected by hydraulic gradient, water quality characteristics, infiltration rates and initial moisture conditions (Huang et al., 1996; Mamedov et al., 2006; Römkens et al., 2002; Shainberg et al., 2003; Zheng et al., 2020).

Cohesion mainly refers to the physicochemical structure that holds the particles together against detachment and rill formation, and this is mechanically considered as a complementary component of the friction forces in the soil (Das, 2008, p. 567), and in general terms, it refers to both physicochemical bonding and frictional forces opposing particle or aggregate removal from the soil matrix (Nouwakpo et al., 2014). Related to that, Nouwakpo et al. (2010) proposed a methodology “fluidized bed approach” to directly measure soil cohesion (C_o). And, they stated that the method had a great potential to directly simulate the behavior of a cohesive material in water, unlike other indirect methods and approaches. In their subsequent research (Nouwakpo & Huang, 2012), they found a strong correlation ($R^2 = 0.82$) between the C_o values and the critical flow shear stress (τ_{cr}) values as the significant variables of the WEPP model to determine the rill erodibility (K_r), experimentally determined by Laflen et al. (1991).

To investigate similar relationships for different soil types, Deviren Saygin et al. (2021) designed an “Automated Soil Cohesion Measurement Apparatus” according to the Fluidized Bed Approach proposed by Nouwakpo et al. (2010) and measured C_o values to test the efficiency of the apparatus with a wide range of soil types in Turkey. In the current study, the goal was to investigate the changes in rill erodibility (K_r) and critical shear stress (τ_{cr}) values as the significant variables of the WEPP model depending on the changes in initial soil moisture conditions, representing dry (air-dried), saturated, and drainage (representing field capacity conditions in terms of soil water contents) moisture levels for these previously sampled soils, which showed higher variations in cohesion properties and internal soil properties. A secondary goal was to evaluate if the soil cohesion (C_o) obtained from fluidized bed approach could be useful in estimating WEPP model rill erodibility parameters. The final goal was to evaluate WEPP model performance with the Nash-Sutcliffe model efficiency for comparison of the measured K_r and τ_{cr} variables under different initial moisture conditions with the predicted K_r and τ_{cr} values from the WEPP model parameterization equations.

2. Materials and methods

2.1. Soils

The soils representing nine different soil texture classes were randomly sampled in two ways, disturbed and undisturbed from 20 different locations at a depth of 0–10 cm with three replicates in the Ayas, Beypazari, and Polatlı districts of Ankara, and in the Karapinar district of Konya located in central Anatolia, Turkey. The soils numbered between 1st and 16th were obtained from Ayas

(1st-4th), Polatli (5th-12th), and the Beypazari (13th-16th) districts in Ankara. The last four soils were sampled from a sand dune area in Karapinar, Konya, Turkey. (Ditzler et al., 2017; Kellogg, 1993). Mean values of measured physicochemical and hydrological soil properties of the tested soils were previously presented by Deviren Saygin et al. (2021) (Tables 1 and 2). The soils represented a wide range of textural compositions including 9 of the 12 major texture classes which were clay (C), clay loam (CL), sandy clay loam (SCL), silty clay (SiC), loam (L), silty clay loam (SiCL), sandy loam (SL), loamy sand (LS), and sand (S) (Ditzler et al., 2017).

2.2. Experimental setup

Rill erodibilities of the soils were evaluated by using a V-shape mini-flume specified by Shainberg et al. (1994). The V-shape flume is a standard flume in terms of its design properties to measure rill erodibility (K_r), and critical shear stress (τ_{cr}) in laboratory conditions.

To measure the rill erodibility (K_r) and critical shear stress (τ_{cr}) in this study, the "Rill Erosion Measurement Setup" was prepared with the V-shaped mini-flumes which could be adjusted for different slope conditions in accordance with the physical framework. For the V-shaped flumes that were portably connected with the assembly, a plexiglass material was used, and 4 flumes with a width of 0.046 m, length of 0.50 m, and depth of 0.12 m, were set at a slope gradient of 3% (Shainberg et al., 1994) (Fig. 1). In order to simulate different soil moisture conditions, the flumes were connected underneath for upward water transmission from their lower parts to the assembly with Mariotte bottles. A sensitive flow meter (FS100A water flow sensor) with an accuracy of ±0.5% was used during the measurements to supply the inflow water (Fig. 1). To obtain different flow conditions and to provide flow control, a water pump with a pumping capacity of 800 L per hour was also included in the system. The water was pumped continuously with the help of a water engine to the water tank with a volume of 20 L placed on the ground through a double bucket (Constant Level Water Reservoir in Fig. 1), which was positioned at a height of 2.35 m, and some of the water was applied to the soil surface in a controlled manner with the precision flow meter.

2.3. Rill erodibility experiments

The Water Erosion Prediction Project (WEPP) model is a widely used tool for predicting soil erosion, particularly from rill and interrill processes. Two key parameters in the WEPP model related to rill erosion are rill erodibility and critical shear stress to calculate the detachment and transport of soil particles in rills. This experiment was designed to provide various levels of flow shear stress to a soil sample and measure the resulting sediment loss.

The soils were placed into the flumes to achieve a natural bulk density similar to a freshly tilled field condition as in Table 1. Three different initial soil moisture conditions were analyzed: (i) dry; soil was initially air-dried, with loose aggregates on the surface similar to seedbed condition (ii) drainage; soil was initially saturated and then excess water was allowed to freely drain away for 24 h through three holes in the flume bottom, until the soil in the flume

Table 1
Basic physicochemical properties of the tested soils (mean values).

Soil no	pH[a]	EC[b]	Lime[c]	SOM[d]	S[e]	Si[f]	C[g]	VCOS[h]	CORS[i]	MEDS[j]	FNES[k]	VFNS[l]	COSI[m]	FNSI[n]	VFSI[r]	TC[o]	BD[p]	PD [q]
1	7.9	0.2	18	2.1	16	39	45	2	1	1	3	8	4	15	11	C	1.2	2.42
2	8.0	0.2	10	2.0	22	35	43	1	1	1	4	16	9	13	4	C	1.1	2.44
3	6.4	0.1	1	1.6	69	14	16	14	7	16	20	12	6	8	2	SL	1.2	2.60
4	7.6	0.5	8	2.5	39	25	36	3	6	7	13	11	6	11	4	CL	1.2	2.49
5	8.1	0.6	17	2.4	15	46	39	1	1	1	4	8	6	23	17	SiCL	1.2	2.46
6	7.9	1.2	24	3.4	19	25	56	0	0	1	3	15	4	17	12	C	1.1	2.41
7	8.1	0.6	16	3.1	11	50	39	0	0	0	2	8	6	19	12	SiCL	1.2	2.45
8	8.1	1.2	18	3.1	20	43	37	0	0	0	3	16	6	17	10	SiCL	1.3	2.47
9	8.1	0.4	22	2.9	16	44	40	1	1	1	4	10	8	23	15	SiC	1.2	2.46
10	7.6	2.5	12	2.2	29	47	24	1	3	5	7	13	4	37	32	L	1.2	2.47
11	8.2	0.4	37	1.5	61	10	29	14	18	10	7	13	2	6	4	SCL	1.0	2.56
12	8.0	0.7	27	3.0	15	29	56	0	0	1	3	11	4	19	15	C	1.2	2.39
13	8.1	0.3	28	1.8	44	29	27	5	8	8	12	11	10	15	4	L	1.3	2.52
14	8.0	0.3	24	3.2	21	36	43	1	1	2	7	10	9	19	11	C	1.2	2.44
15	7.7	0.8	24	2.1	19	32	49	1	1	1	5	11	6	17	11	C	1.2	2.43
16	8.1	0.2	27	2.6	19	39	43	1	2	2	6	9	13	24	11	C	1.2	2.44
17	8.8	0.1	46	0.1	97	1	2	0	6	53	38	2	0	0	0	S	1.6	2.66
18	8.7	0.1	52	0.7	92	4	4	0	1	13	66	12	2	2	0	S	1.6	2.64
19	8.4	0.2	52	1.2	84	10	6	0	1	18	40	24	6	10	4	LS	1.5	2.62
20	8.3	0.2	45	1.7	80	10	10	2	5	12	45	16	6	6	0	LS	1.5	2.61

[a] Soil reaction (Richards, 1954).
[b] Electrical conductivity (dS m^{-1}) (Richards, 1954).
[c] Calcium carbonate (%) (Caglar, 1958).
[d] Soil organic matter (%) (Nelson & Sommers, 1982).
[e] Sand (2–0.05 mm) (%).
[f] Silt (0.05–0.002 mm) (%).
[g] Clay (<0.002 mm) (%).
[h] Very coarse sand (2-1 mm) (%).
[i] Coarse sand (1–0.5 mm) (%).
[j] Medium sand (0.5–0.25 mm) (%).
[k] Fine sand (0.25–0.1 mm) (%).
[l] Very fine sand (0.1–0.05 mm) (%).
[m] Coarse silt (0.05–0.02 mm) (%).
[n] Fine silt (0.02–0.002 mm) (%).
[o] Texture classes.
[p] Bulk density (g cm^{-3}) (Richards, 1954).
[q] Particle density (g cm^{-3}) (Blake & Hartge, 1986).
[r] Very fine silt content (0.002–0.005 mm) (%).

Table 2
Some physical and hydrologic properties of the tested soils (mean values).

Soil no	Soil moisture content (%) (v/v)[a]						Co [b]	V_f[c]	WSA[d]	HC [e]	MWD[f]	P[g]	LL[h]
	Air dried	pF 0 (saturated)	pF 1.7	pF 2	pF 2.54 (Field capacity)	pF 4.2 (Permanent wilting point)							
1	7.97	88.14	83.73	65.53	51.08	32.48	49	0.025	44	6	2.73	88	51
2	8.77	84.31	78.16	61.34	50.13	31.14	11	0.048	44	7	2.26	85	53
3	2.77	51.24	46.76	39.19	25.86	13.36	16	0.025	56	9	2.56	51	23
4	6.01	80.76	74.11	58.76	46.16	25.91	27	0.027	52	5	3.32	81	43
5	3.65	60.68	53.51	47.53	43.78	23.00	212	0.003	71	2	2.26	61	38
6	4.04	70.01	66.16	50.17	41.19	27.01	87	0.011	74	5	3.23	70	46
7	3.18	61.32	53.23	46.80	39.87	22.24	107	0.003	59	1	2.55	61	37
8	3.26	59.50	32.05	44.72	38.94	23.00	145	0.003	39	1	2.70	60	37
9	4.60	70.86	62.51	53.41	46.00	25.41	212	0.005	78	2	2.76	71	37
10	7.92	66.85	57.76	52.73	48.72	27.91	151	0.007	83	17	2.43	67	32
11	3.32	64.66	64.51	46.46	36.68	21.80	51	0.014	79	13	2.61	65	26
12	4.03	74.51	67.85	51.36	40.52	24.48	161	0.005	81	5	3.80	74	43
13	4.04	63.95	56.24	50.04	40.47	18.69	88	0.005	59	29	2.18	64	29
14	6.70	85.62	79.78	65.94	52.22	26.92	140	0.008	56	7	1.88	86	54
15	6.39	73.77	66.92	61.48	54.86	26.88	164	0.006	50	5	1.86	74	51
16	7.12	91.55	83.32	65.54	52.08	29.51	146	0.008	59	9	1.79	92	49
17	0.51	38.39	36.04	11.96	7.70	4.46	26	0.010	*	66	0.32	38	*
18	0.91	44.83	41.31	33.36	9.45	5.54	5	0.043	*	26	0.22	45	*
19	1.25	61.37	57.10	49.88	21.40	9.55	29	0.036	*	18	0.23	61	*
20	1.23	54.85	49.63	44.58	19.16	9.03	32	0.048	*	10	0.14	55	*

pF = log 10 of soil water tension.
* Reliable data could not be obtained because these samples, which have a very high sand content, do not have sufficient structural strength in terms of the mentioned properties.
[a] Soil water contents (%) (v/v) at air dried, pF 0 (saturated), pF 1.7, pF 2, pF 2.54 (field capacity) and pF 4.2 (permanent wilting point) (Richards, 1954).
[b] Cohesion (kPa m^{-1}) (Nouwakpo et al., 2010).
[c] Flow velocity at fluidization (m s^{-1}) (Nouwakpo et al., 2010).
[d] Water stable aggregates (%) (Kemper & Rosenau, 1986).
[e] Hydraulic conductivity (cm h^{-1}) (Klute & Dirksen, 1986).
[f] Mean weight diameter (mm) (dry sieving) (Kemper & Rosenau, 1986).
[g] Soil porosity (%).
[h] Liquid limit (%) (Bowles, 1992).

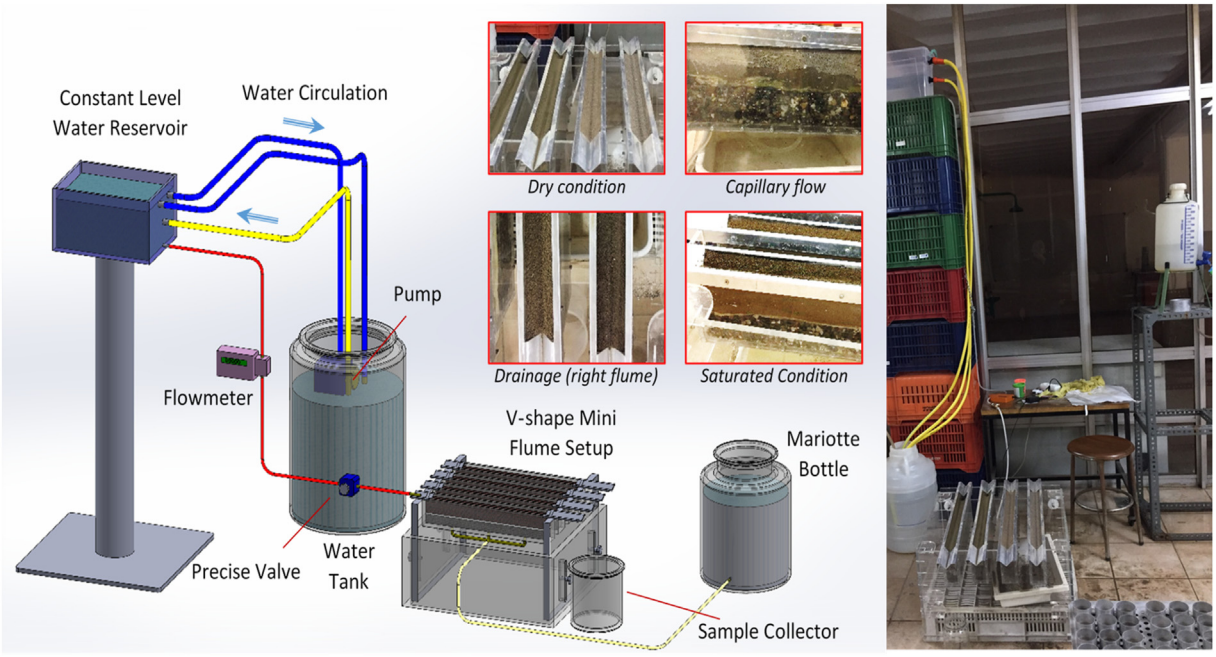

Fig. 1. Schematic view of rill erodibility setup and experiments.

retained all water it could against the force of gravity, and (iii) saturation; soil was saturated from the bottom by capillarity through the holes in the flume's bottom. Water added to saturation was stopped when the water reached the soil surface and when a water film was seen around the surface particles before runoff could begin. Then, the upward water flow was cut off by plugging the flume bottom holes.

In the experiments, deionized water was introduced at the top of the flume, and the inflow rate was controllable and measured using the flow-meter from 0.10 L min^{-1} to 0.65 L min^{-1} in Fig. 1.

During an experiment, the flow rate was increased in 0.05 L min^{-1} increments, and in total 12 flow rates were tested. The specified flow rates were gradually reached without any interruptions until the final flow level was reached. For each flow rate, runoff samples with three replicates were collected and weighed, after which they were oven-dried at 105 °C. Thus, runoff volume and sediment concentrations were determined gravimetrically. As a result, a total of 6480 runoff and runoff sediment samples were obtained for all tested conditions and soils, and the rill erodibility (K_r) and critical flow shear stress (τ_{cr}) values of the soils were determined using the WEPP model approach.

In the WEPP model, net soil detachment in rills is calculated for the case when flow hydraulic shear stress (τ) exceeds the critical shear stress (τ_{cr}) of the soil and when sediment load is less than sediment transport capacity. The relationship between detachment and erodibility is given in Eq. (1).

$$D_c = K_r(\tau - \tau_{cr}) \tag{1}$$

where D_c is the rill detachment capacity rate (kg m^{-2} s^{-1}); K_r is the rill erodibility (kg m^{-2} s^{-1}); τ is the flow shear stress (Pa), and τ_{cr} is the critical flow shear stress (Pa) (Foster et al., 1995). Flow shear stress was obtained with Eq. (2).

$$\tau = \gamma R_h S \tag{2}$$

where γ is the specific weight of water (N m^{-3}); R_h is the hydraulic radius of the flow (m); and S is the slope gradient of the rill channel (m m^{-1}).

In Eq. (2) the hydraulic radius (R_h) was derived from the Manning's equation which depends upon the rill shape. In this study two rill shapes, which were V-shaped (Eq. (3)) and semicircular-shaped (Eq. (4)), were observed from the beginning to the end of the flume experiments.

$$R_h = \frac{1}{2^{1.5}}\left(\frac{2nQ}{S^{1/2}}\right)^{3/8} \tag{3}$$

$$R_h = \frac{1}{2}\left(\frac{2^{5/8}nQ}{\pi S^{1/2}}\right)^{3/8} \tag{4}$$

where n is the Manning roughness coefficient; and Q is the flow rate (m^3 s^{-1}) (Shainberg et al., 1994).

The critical flow shear stress (τ_{cr}) of the tested soils was obtained from the linear relationship between the detachment rate and the flow shear stress values. In the linear regression, the slope of the line is the rill erodibility, and the point where the line intersects with the X-axis (flow shear stress) gives the critical flow shear stress.

The observed datasets were explicitly tested for normality (Kolmogorov-Smirnov), and homogeneity of variance (Levene's test) before conducting comparison analyses. The test results for the K_r and τ_{cr} values were then statistically evaluated using the general linear model analysis (multivariate) of variance (ANOVA) and the LSD test with twenty soil types and three moisture contents, and the significance level of differences between averages was compared using "IBM SPSS Statistics 22 and MSTAT-C". Pearson correlation analysis was also performed to determine paired correlations on some soil parameters.

2.4. Model performance with Nash-Sutcliffe model efficiency

WEPP model performance was evaluated using the Nash-Sutcliffe model efficiency (NSE; Nash & Sutcliffe, 1970) for comparison of the measured K_r and τ_{cr} variables under different initial moisture conditions with the predicted K_r and τ_{cr} values from the WEPP model parameterization equations (Eq. (6) - Eq. (9)). NSE evaluates the relationship between features obtained by various models and those obtained through measurement (Eq. (5)). Briefly, this approach is a normalized statistical method used to measure the accuracy of many hydrological predictions. The most important reason for the effectiveness of NSE in method performance measurement is that it is the function that best represents the overlap in measured and predicted data (Lin et al., 2017; McCuen et al., 2006; Srivastava et al., 2017).

$$NSE = 1 - \frac{\sum (Y_m - Y_p)^2}{\sum (Y_m - Y_{mean})^2} \tag{5}$$

where Y_m is the measured value, Y_p is the value predicted by the model, and Y_{mean} is the measured mean.

The measured K_r and τ_{cr} values were compared to values obtained using the default WEPP model parameterization equations (Alberts et al., 1995; Flanagan & Livingston, 1995). The equations for cropland surface soils containing 30% or more sand content are:

$$K_r = .00197 + .00030VFS + .03863e^{-1.84OM} \tag{6}$$

$$\tau_{cr} = 2.67 + 0.065C - 0.058VFS \tag{7}$$

For cropland soils containing less than 30% sand, the equations are:

$$K_r = .0069 + .134e^{-.20C} \tag{8}$$

$$\tau_{cr} = 3.5 \tag{9}$$

where *VFS* is the very fine sand content (%), *C* is the clay content (%), and *OM* is the soil organic matter content (%). The *VFS* value must be less than or equal to 40%, and if it is greater than 40%, it is assumed to be 40% in this equation application. The *OM* must be greater than 0.35%, and if it is less than 0.35%, it is set at 0.35%. *C* must be greater than 10% and less than 40%, and if it is less than 10%, it is set at 10%, and if it is greater than 40%, it is set to be 40%.

3. Results

3.1. Effects of changing initial soil moisture conditions on rill erodibility and critical shear stress

Findings revealed that the variations in moisture contents and soil types have statistically significant effects on the K_r and τ_{cr} values ($P < 0.01$) and there was an interaction between moisture conditions and the soil type ($P < 0.01$) (Table 3).

Figs. 2 and 3 graphically illustrate the Fisher's least significant difference test (LSD) comparisons of the measured K_r and τ_{cr} values of the soils in terms of the tested initial moisture contents. Generally, statistically significant changes in rill erodibilities were noticeably observed in fine-textured soils compared to coarse-textured ones, depending on the changes in initial moisture conditions. Although critical flow shear stress of the soils presented a less noticeable change compared to the rill erodibilities when their textural properties are taken into account, τ_{cr} values in sandy soils were chiefly found to be greater.

In the experiments where the initial moisture condition was dry, the greatest K_r value was obtained for the 4th soil, which has a clayey loam texture, while the lowest was obtained for the 18th soil, sampled from a sand dune in Karapinar, Konya (Fig. 2). In terms of

Table 3
Analysis of variance for measured K_r (s m^{-1}) and τ_{cr} (Pa) values.

Source	Dependent Variable: K_r					Dependent Variable: τ_{cr}				
	Type III Sum of Squares	df	Mean squares	F	P	Type III Sum of Squares	df	Mean squares	F	P
Corrected Model	0.010 [a]	59	0.000	67.228	0.000	1.029 [a]	59	0.017	14.656	0.000
Intercept	0.007	1	0.007	2599.794	0.000	33.199	1	33.199	27893.823	0.000
Moisture	0.003	2	0.001	535.320	0.000	0.050	2	0.025	21.109	0.000
Soil	0.004	19	0.000	84.922	0.000	0.411	19	0.022	18.154	0.000
Moisture * Soil	0.003	38	8.813E-05	33.745	0.000	0.568	38	0.015	12.568	0.000
Error	0.000	120	2.612E-06			0.143	120	0.001		
Total	0.017	180				34.371	180			
Corrected Total	0.011	179				1.172	179			
LSD	0.0082					LSD	0.0511			
[a] R Squared = 0.971 (Adjusted R Squared = 0.956)						[a] R squared = 0.915 (Adjusted R Squared = 0.873)				

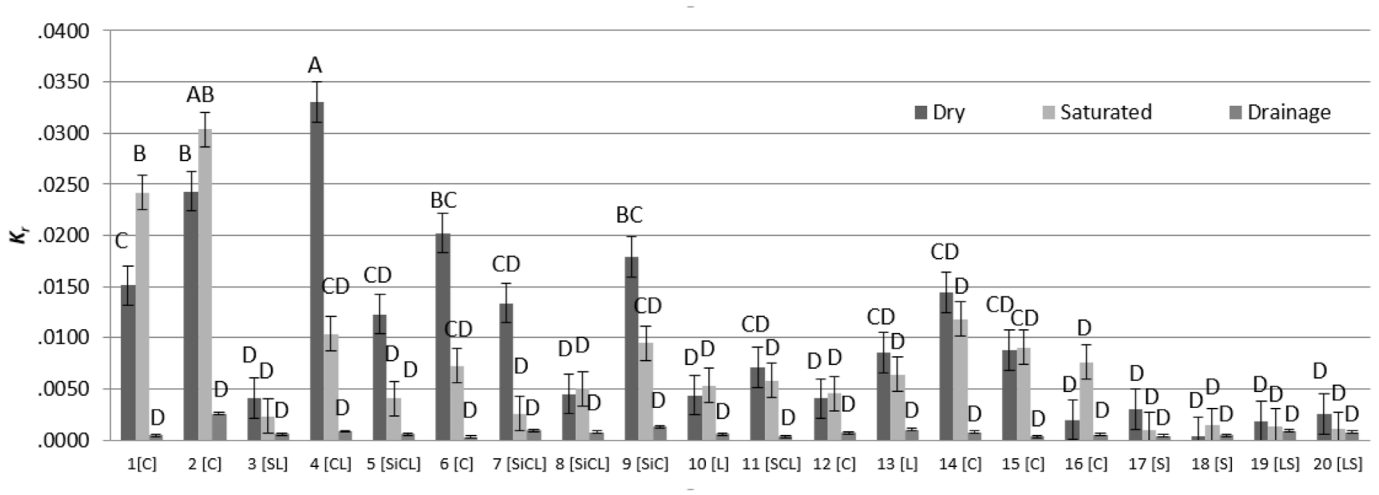

Fig. 2. Statistical comparison of the K_r (s m^{-1}) values derived in terms of initial moisture contents for the 20 test soil types presented in the x-axis with abbreviated texture classes. Data are the mean (±SE) values of the K_r values. In the graph, means with different capital letters were significantly different in terms of their K_r values ($p < 0.05$; LSD: 0.0082).

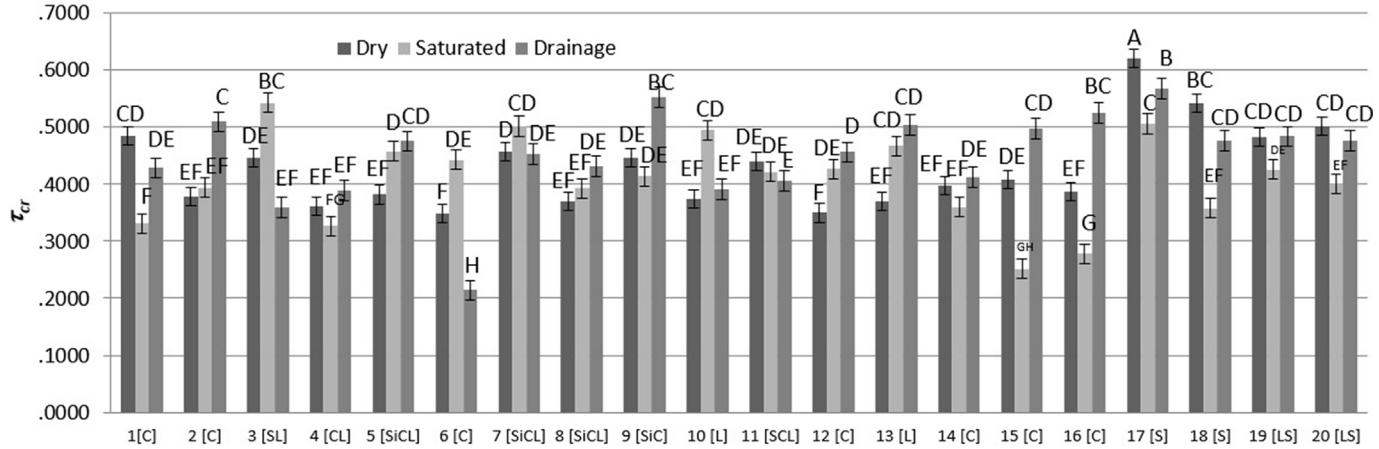

Fig. 3. Statistical comparison of the τ_{cr} (Pa) values derived in terms of initial moisture contents for the test soil types. Data are the mean (±SE) values of the τ_{cr} values. In the graph, means with different capital letters were significantly different in terms of their τ_{cr} values ($p < 0.05$; LSD: 0.0511).

critical flow shear stresses, the lowest τ_{cr} was measured for the 6th soil, which has the highest clay content among the studied soils. The greatest τ_{cr} value was obtained for the 17th soil taken from dune field and it had the highest sand content (97%) among the studied soils (Fig. 3).

In the saturated conditions, the sandy-textured 17th soil had the lowest K_r values. The greatest K_r value was measured for the clay-textured 2nd soil for this condition (Fig. 2). In terms of τ_{cr}, the 3rd soil had the greatest value (0.54 Pa), which was also rich in sand content (69%). The lowest τ_{cr} value of 0.25 Pa was obtained for the 15th soil, having 49% clay content (Fig. 3). Findings suggested that clay-rich soils, when the initial conditions were saturated, could be

easily detached and transported in the rill under lower flow shear stresses compared to the coarse-textured soils.

When the soils were kept under free drainage conditions for 24 h after being saturated, no statistically significant differences were observed in K_r values for all the tested soils (Fig. 2). However, the τ_{cr} values significantly changed for the tested soils under drainage conditions ($P < 0.01$). The greatest τ_{cr} value was obtained for the 17th soil sampled from the sand dune, while the lowest was obtained for the clay-rich 6th soil (Fig. 3).

The soils were also separated into three subgroups to better visualize the K_r and τ_{cr} variations in terms of the tested initial moisture contents and comparison of them with the predicted K_r and τ_{cr} values from the WEPP model parameterization equations according to the dominant textural compositions as Clayey (1 [Clay], 2 [Clay], 6 [Clay], 12 [Clay], 14 [Clay], 15 [Clay], 16 [Clay]); *Silty* (5 [Silty clay loam], 7 [Silty clay loam], 8 [Silty clay loam], 9 [Silty clay], 10 [Loam]); and, *Sandy* (3 [Sandy loam], 4 [Clay loam], 11 [Sandy clay loam], 13 [Loam], 17 [Sand], 18 [Sand], 19 [Loamy sand], 20 [Loamy sand]), respectively (Figs. 4 and 5).

Similar to Figs. 2 and 4 indicates that rill erodibility in clay-rich soils generally increased under saturated conditions, but this wasn't always the case for all soils. For most clay-rich soils, rill erodibility was greater when the soils were saturated compared to when they were dry. This could be due to the reduced cohesion and increased pore pressure in saturated soils, making them more susceptible to erosion. However, most of the tested clay-rich soils did not exhibit a significant change in rill erodibility when comparing dry and saturated conditions with the exception of the 1st soil (Fig. 2). This suggests that for this soil, moisture content alone may not be the dominant factor influencing its susceptibility to rill erosion. Overall, while moisture content typically influences erodibility, the lack of significant change in K_r for most soils in the study suggested that other factors such as particle size distributions, structure or organic content might play a more crucial role in controlling rill erodibility in these clay-rich soils.

Across all soil samples, the lowest rill erodibilities were observed under the drainage conditions. This suggests that when excess water is removed, soil stability improves, making it less prone to erosion. In some clay-rich soils e.g. 1st and 2nd (Fig. 2.), the decrease in rill erodibility under drainage conditions was statistically significant. It is thought that clay-rich soils may be particularly responsive to drainage, likely because the removal of water reduces

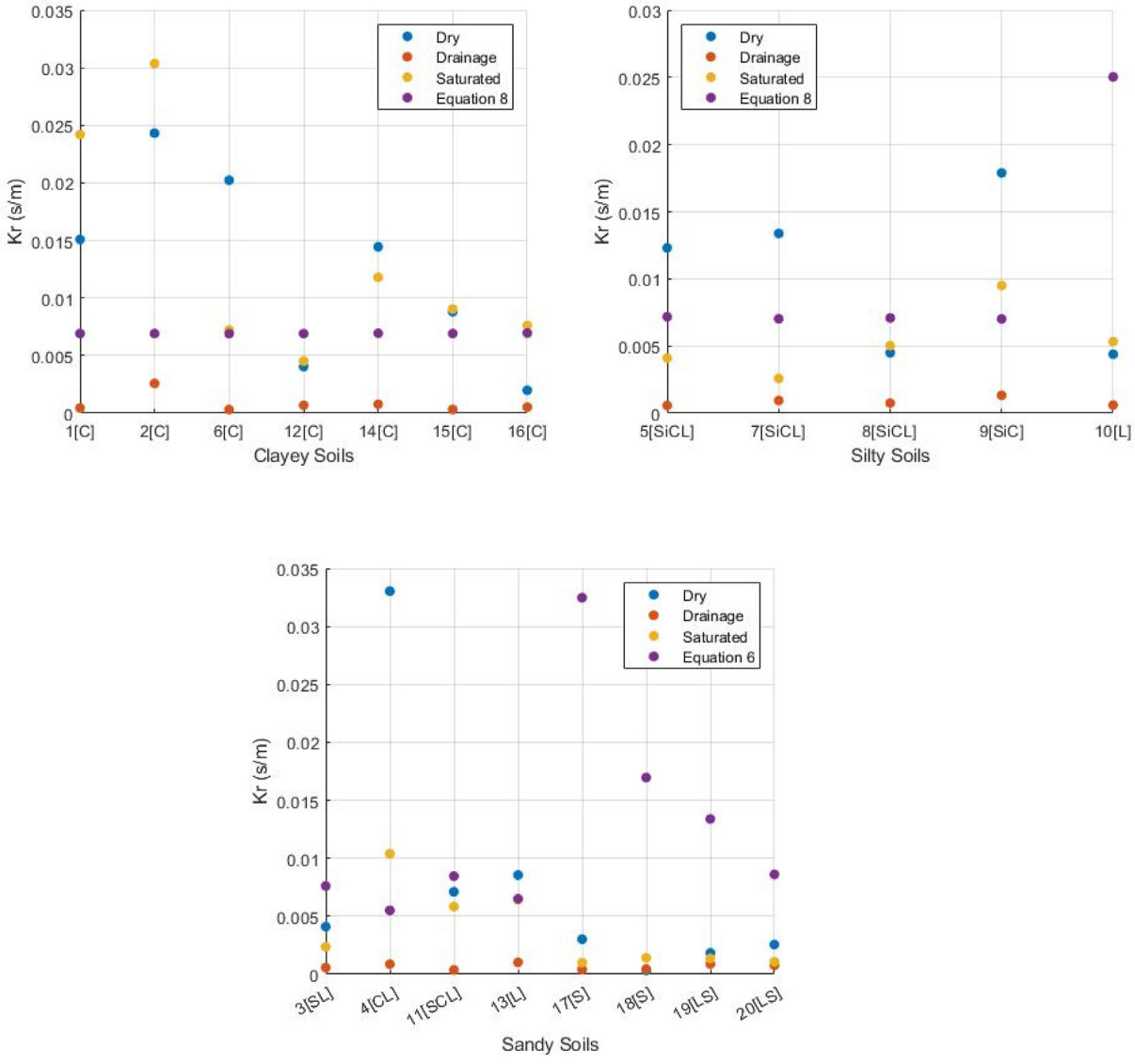

Fig. 4. Clustering K_r values based on the dominant textural composition of the soils.

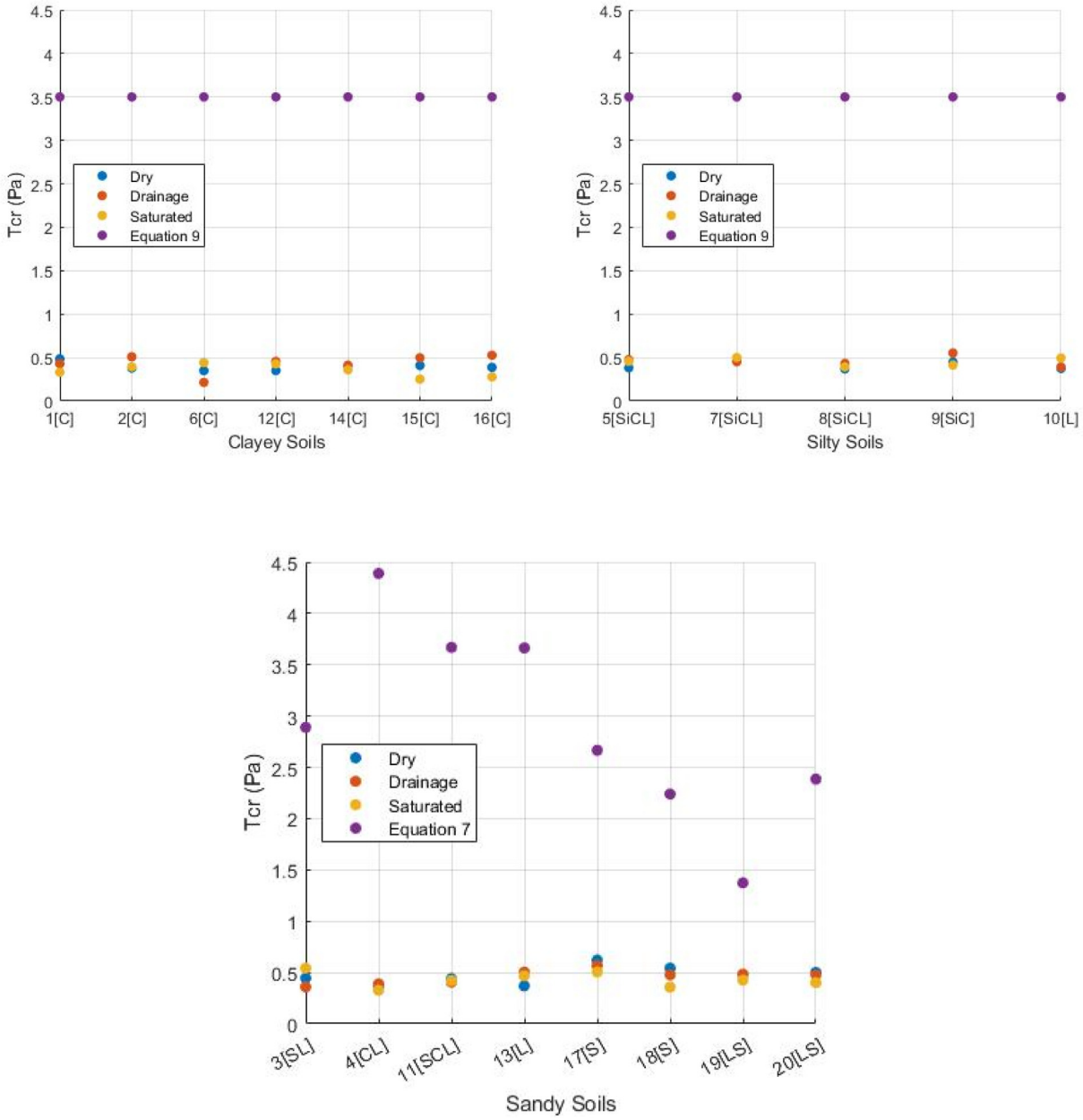

Fig. 5. Clustering τ_{cr} values based on the dominant textural composition of the soils.

the swelling and dispersion of clay particles, which otherwise could weaken the soil structure and increase erodibility. In contrast, soils dominated by silt and sand did not show a statistically significant change in rill erodibility under drainage conditions compared to other moisture conditions, except for soil #4. This could be because silt and sand particles are less affected by changes in moisture content compared to clay particles, leading to more stable erodibility rates regardless of drainage. The effectiveness of drainage in reducing rill erodibility could be strongly dependent on the clay content of the soil. While drainage significantly improved the stability of clay-rich soils, its impact could be less pronounced in coarse-textured soils where silt and sand were the dominant components.

Observations revealed important insights into the relationship between critical flow shear stress (τ_{cr}) and rill erodibility (K_r), and how these properties varied depending on soil texture and moisture conditions. The highest critical shear stress values were typically observed under dry conditions in soils with high sand contents (Fig. 3). Sandy soils typically have greater hydraulic conductivity values due to the larger pore spaces between particles, which allows for easier water infiltration and reduces surface runoff. This, in turn, leads to a decrease in sediment detachment rates. Conversely, in soils with high clay content, the highest τ_{cr} values were generally measured under drainage conditions. This could be likely due to the cohesive nature of clay particles, which become more stable and resistant to erosion once excess water is drained, enhancing the soil's critical shear stress. In other words, soils that require higher shear stress to initiate erosion tend to be less erodible. While the general trend aligns with expectations such as higher τ_{cr} corresponds with lower K_r, not all soils exhibited statistically significant changes in these parameters in terms of initial moisture conditions. This suggested that while the

relationship holds true on a broad level, other factors might influence erodibility in certain soils, leading to variability that wasn't always statistically significant.

3.2. WEPP model parameterization equation evaluations

The soils having greater silt contents mostly had higher NSE values for both the initially dry and saturated conditions (Table 4). Thus, K_r values measured under these conditions, especially for some soils, were in better agreement with those estimated from the baseline equations in the WEPP model (Fig. 4). For the initially dry soil conditions, the estimated efficiency values were greater for the 3rd (sandy loam), 5th (silty clay loam), 11th (sandy clay loam), 12th (clay), 13th (clay loam) and 14th (clay) soils and the best performance (NSE: 1) was for the 8th soil, which has a silty clay loam structure. For the saturated conditions, the predicted and measured WEPP-K_r variables had higher NSE values for the 8th (silty clay loam), 9th (silty clay), 11th (sandy clay loam), 12th (clay), 13th (clay loam), 14th (clay), 15th (clay) soils. The highest model efficiency under these conditions was for the 6th soil (NSE: 0.99), which has the greatest clay content (56%) among the studied soils. This was also consistent with the conditions under which the WEPP model parameterization equations were developed. Comparatively, the τ_{cr} values obtained under laboratory conditions with the v-shaped mini-flume setup were usually lower than the values predicted by the baseline model parameterization equations (Fig. 5). All NSE values for the computed critical shear stress versus measured values were negative and, therefore, were not included in Table 4.

3.3. Relationships between soil properties and rill erosion

Pearson correlation analysis was carried out in order to reveal the relationships between soil characteristics including soil cohesion measurements with rill erodibility and other associated variables for all soil data (n = 60 with replicates) (Fig. 6). Additionally, the soils were evaluated in two groups, soils containing 30% or more sand (n = 24 with replicates) (Fig. 7) and soils containing less than 30% sand (n = 36 with replicates) (Fig. 8) in accordance with the WEPP model parameterization equations.

When analyzing the data as pooled, significant correlations were generally observed between particle size distribution, soil organic matter contents and porosity variables, and both rill erodibility (K_r) and critical flow shear stress (τ_{cr}), especially under dry conditions.

In soils containing 30% or more sand, no significant correlation was observed between rill erodibility, critical flow shear stress, and the C_o and V_f values under any tested moisture conditions (Fig. 7). This indicated that in these tested sandy soils, cohesion and flow properties could be less influential in determining erodibility and shear stress resistance. However, significant correlations were found among rill erodibility, critical flow shear stress, and particle size distributions e.g. COSI, FNSI, VFSI, silt, clay, sand contents under dry and saturated conditions for soils containing 30% or more sand. Typically, an increase in SOM is expected to enhance soil structure and reduce erodibility, but in these sandy soils unexpected positive correlations between soil organic matter (SOM) and rill erodibilities for all tested moisture contents were observed.

In soils containing 30% or less sand, there were significant and strong correlations between cohesion (C_o) and flow velocity at fluidization (V_f) values with rill erodibility, particularly under saturated conditions. This revealed that in these clay-rich soils, the greater the cohesion resulted in lower rill erodibilities (Fig. 8). And, the cohesion and flow velocity measured at the fluidization point could have a potential in determining the soil's susceptibility to rill erosion when saturated.

Table 4
Nash-Sutcliffe model efficiencies (NSE) for equation-predicted versus measured rill erodibilities and critical shear stress values for the 20 tested soils. NSE values greater than zero are highlighted in bold font.

Soil [Texture class]	$K_{r\ [dry]}$	$K_{r\ [saturated]}$	$K_{r\ [drainage]}$
1[C]	−18.64	−173.3	−55780
2 [C]	−170000	−10.19	−46.26
3 [SL]	**0.43**	−0.69	−1437
4 [CL]	−1.36	−1.01	−100.0
5 [SiCL]	**0.61**	−55.52	−516.3
6 [C]	−0.10	**0.99**	−341.8
7 [SiCL]	−34.47	−7.62	−71.02
8 [SiCL]	**1.00**	**0.10**	−158.4
9 [SiC]	−4.86	**0.78**	−901900
10 [L]	−5010	−2466	−30690
11 [SCL]	**0.32**	**0.48**	−2681
12 [C]	**0.99**	**0.77**	−102.1
13 [L]	**0.90**	**0.96**	−106.8
14 [C]	**0.44**	**0.40**	−1033.
15 [C]	−0.22	**0.37**	−1105.
16 [C]	−4.67	**0.78**	−239.2
17 [S]	−1721000	−148100	−92410
18 [S]	−49200	−543400	−33620
19 [LS]	−100000	−42570	−25830
20 [LS]	−75900	−142400	103100

4. Discussion

4.1. Changing initial soil moisture conditions and their effects on the K_r and τ_{cr} values

Overall findings from this study have clearly confirmed results of previous studies where many authors found that initial soil water content affects soil erodibility under concentrated flow, and there was an inverse relationship between erodibility and critical flow shear stress values (Govers, 1991; Govers et al., 1990; Grissinger et al., 1981; Kemper et al., 1985; Nachtergaele & Poesen, 2002). It is generally thought that an increase in initial moisture conditions results in greater erodibilities due to a decrease in the cohesive forces that hold the particles together (Knapen et al., 2007; Nachtergaele & Poesen, 2002; Van Klaveren & McCool, 1998; Yu et al., 2014). It is also thought that soils develop maximum cohesive strength under drainage conditions, which causes soils to be less erodible for detachment within a rill compare to dry conditions (Deviren Saygin et al., 2018; Grissinger, 1966, 1972; Hanson et al., 1999; Knapen et al., 2007; Shainberg et al., 1996).

However, the effect of changes in soil moisture conditions is complex on the erodibility potential of soils (Shainberg et al., 1996). In some cases where soil moisture content is low such as clay-rich soils under dry conditions, soil particles cannot move easily enough to direct themselves to a position with high cohesion due to low energy levels. This can lead to lower rill erodibilities (Knapen et al., 2007; Shainberg et al., 1996). The 1st and 2nd soils here could be best-fit examples for this phenomenon (Figs. 2 and 4).

Increases in initial moisture contents (e.g., saturated or seepage conditions) lead to increases in sediment discharge rates compared with the drainage conditions in terms of vertical hydraulic gradients. Our results are similar to other relevant studies reported by several researchers from past to present (Deviren Saygin et al., 2018; Huang & Laflen, 1996; Römkens et al., 2002; Zheng et al., 2000). Similarly, among all the studied soils, the lowest K_r values were obtained for the drainage conditions where there was sufficient wetting and drying for cohesion development, while the greater erodibilities were mostly observed under the initially dry soil condition (Figs. 2 and 4).

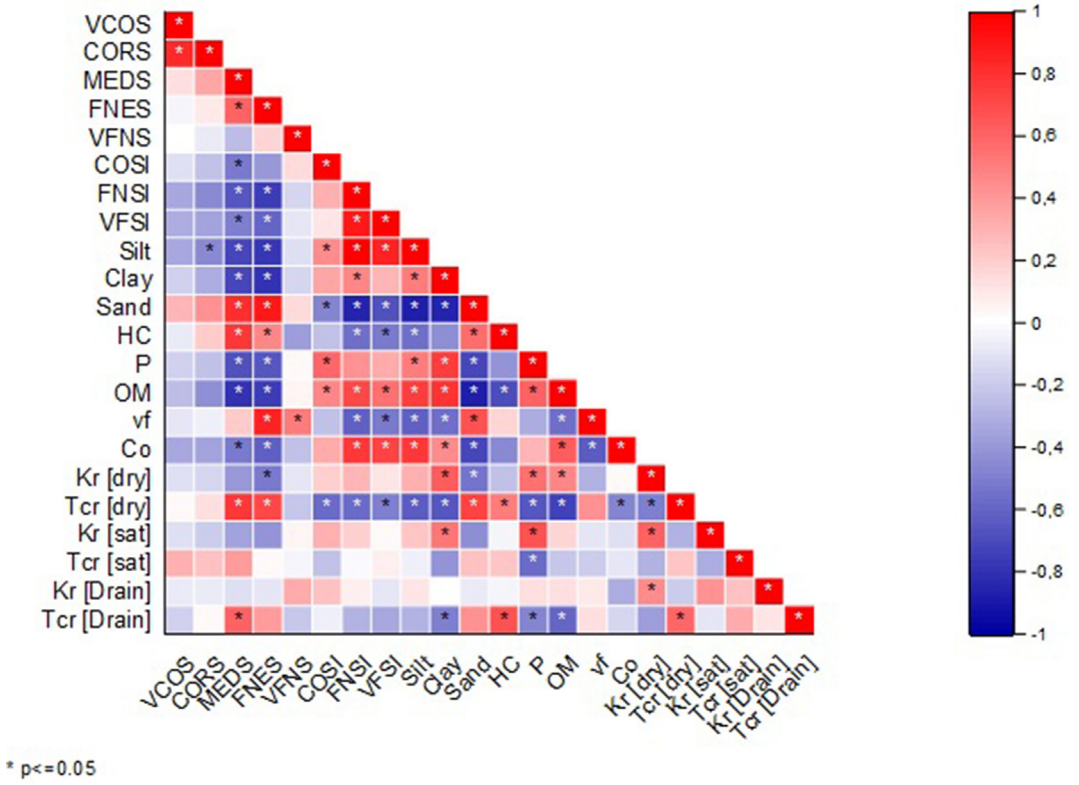

Fig. 6. Correlation matrix between soil properties and K_r and τ_{cr} values in terms of initial soil moisture conditions for pooled data (including all soil types).

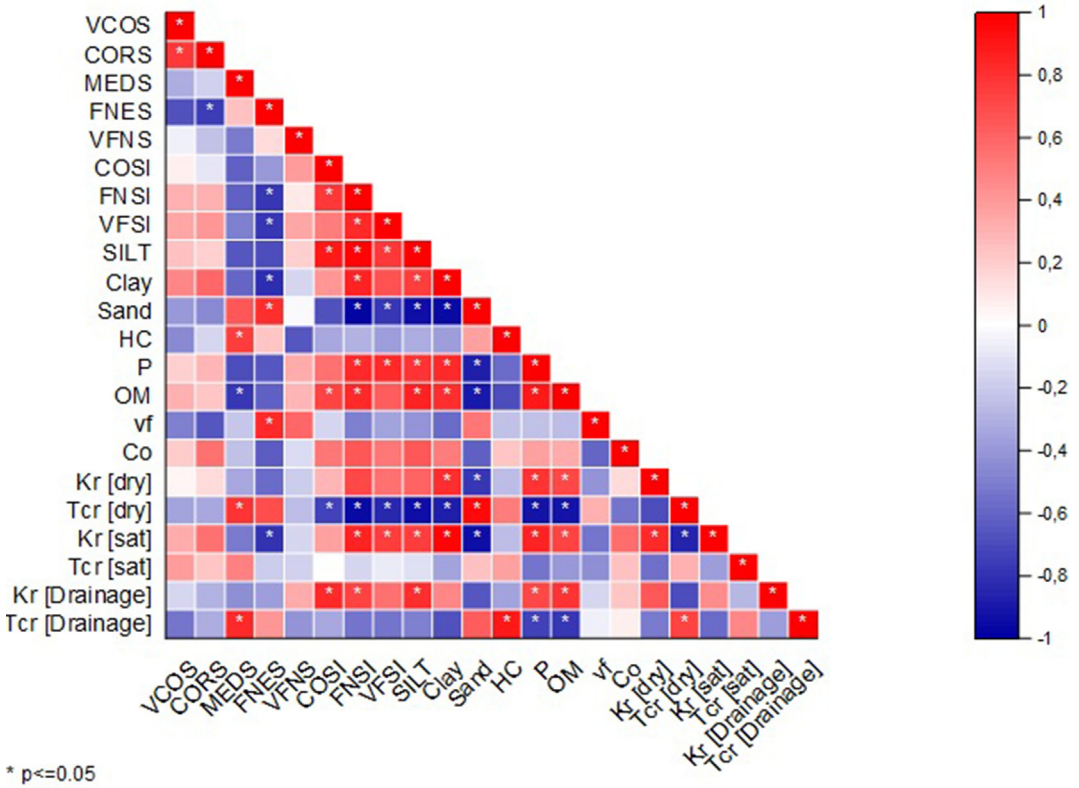

Fig. 7. Correlation matrix between soil properties and K_r and τ_{cr} values in terms of initial soil moisture conditions for soils containing 30% or more sand.

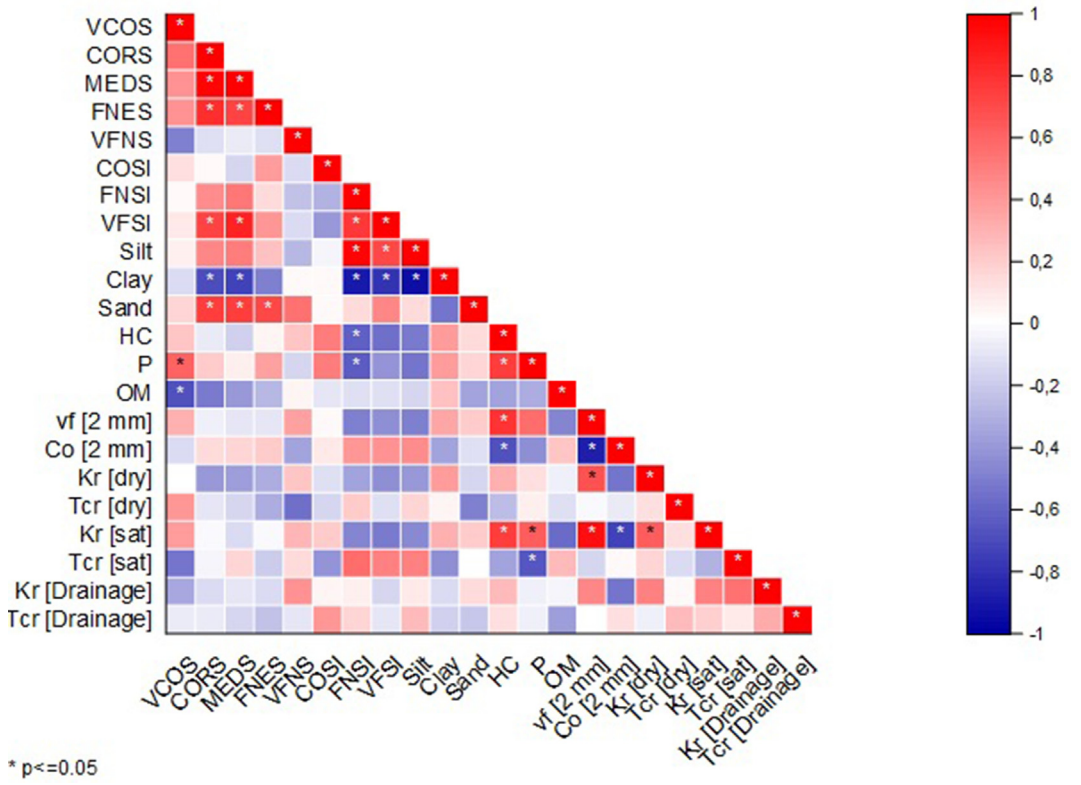

Fig. 8. Correlation matrix between soil properties and K_r and τ_{cr} values in terms of initial soil moisture conditions for soils containing less than 30% sand.

Bryan & Rockwell (1998) found sediment concentration rates increased by approximately 30 times when the water table was present at the soil surface, theoretically reaching the saturation point. What we do know today is that erodibility potential of a soil in a channel is governed by cohesion between the solid particles and the consolidation degree, and directed by flow velocity and particle size distribution (Schieber, 2011). Nouwakpo et al. (2010) found that the presence of positive pore pressure near the soil surface was a major factor in reducing soil cohesion. This confirms greater erodibility potential of the soils under saturated conditions, especially for fine-textured soils. Comparing tested soil moisture conditions, almost all of the clay-rich soils had greater τ_{cr} values under drainage conditions (Fig. 3). This indicated that the soils rich in clay content had greater resistance to detachment under drainage conditions. However, erodibility potentials of the soils under initially dry conditions in silt-rich soils were at least as high as those in saturated conditions (Fig. 2).

Considering the studied sandy soils which originated from sand dunes e.g 17th-20th soils, they often displayed characteristics that distinguished them from the other coarse-textured soils. The sand in dunes tends to be well-sorted, meaning the particles are relatively uniform in size. This is because the wind processes often sort the particles during dune formation. Thus, dunes typically have a low capacity to form stable soil aggregates due to their coarse texture and lack of binding materials such as organic matter or clay. This makes them less cohesive. Despite their low aggregation, sand dunes have a high infiltration capacity. The other tested sandy soils had a broader range of particle sizes, including some finer materials like silt or clay. The large pore spaces between the sand particles allow water to percolate through the soil more quickly than in finer-textured soils (Table 1). Therefore, these soils cannot be easily mobilized and transported under shallow surface flow conditions compared to fine-textured soil types, and this was confirmed with the greater τ_{cr} values of these soils that were obtained for all experimental moisture conditions. However, the fine-textured soils could be readily fragmented and transported under lower flow shear stress values despite their greater cohesive potential (Erpul et al., 2013; Tsoar, 2005) (Fig. 5).

4.2. WEPP model parameterization equation evaluations

In terms of the calculated NSE values (Table 4), the rill erodibility (K_r) values measured under drainage conditions, and the τ_{cr} values measured under all moisture conditions showed very low agreement with the data estimated by the WEPP model baseline parameterization equations (Fig. 5). This indicates that measurements obtained from the mini-flumes under drainage conditions for the studied soils did not agree with the values estimated by the baseline model equations, and that the performance of the WEPP model equations in reflecting the changes in initial hydrological conditions on sediment losses is limited. However, as the WEPP equations were developed from field studies conducted mostly on initially dry or saturated soil conditions for silt-dominated soil types, one would not expect them to perform well under drained conditions such as in this study.

Another reason for this tendency has to do with the experimental setup in this small-scale lab study, compared to the larger-scale WEPP field rainfall simulation experiments using rills that were 9 m long on 0.46 m spacings (Elliot et al., 1989). The field study also had much larger and, in many cases, more stable aggregates where the data for the baseline WEPP equations were obtained, compared to the much smaller setups and smaller and more uniform soil aggregate structure under our laboratory conditions (Deviren Saygın et al., 2018).

As noted by Nearing et al. (1990), the equations developed to assess baseline rill erodibility values in the WEPP model, relying on

internal soil properties, often suffer from high error rates and uncertainties. This was attributed to limited data availability and sample groups exhibiting significant variation. Similarly, Brunner et al. (2004) highlighted the WEPP model's sensitivity to changes in soil texture, particularly in terms of hydraulic property calculations.

Exemplarily, in the initially saturated soil conditions, clay-rich soils especially had better agreements compared to the other tested moisture conditions. For the initially drained conditions, these clay-rich soils tended to form more durable aggregates (Kemper & Rosenau, 1984), reducing the susceptibility of these soils to erosion, leading to a significant decrease in overland flow-induced detachment and sediment transport (Mamedov et al., 2006; Moutier et al., 1998; Nouwakpo et al., 2014; Shainberg et al., 1996).

Several studies have emphasized the need for more diverse field experiments within the framework of the WEPP model, particularly focusing on internal soil properties. This necessity becomes apparent, especially for soils with particle size distributions differing from silt-dominated soil groups (Brubaker et al., 1992; Flanagan & Nearing, 2000; Wang et al., 2023; Zhang et al., 2005). By conducting extensive field and laboratory experiments across various soil types, the model's performance can be enhanced. This entails verifying and potentially adjusting the erodibility parameterization equations based on empirical measurement results.

In summary, addressing these recommendations for broader and more comprehensive data collection and model validation efforts can significantly contribute to refining the accuracy and applicability of the WEPP model in predicting rill erosion dynamics across diverse soil types and hydrological conditions.

4.3. Relationships between soil properties and rill erosion

Some relevant studies stated that rill erodibility declines as soil organic matter (SOM), clay, and MWD increase (Alberts et al., 1995; Chenu et al., 2000; Deviren Saygin et al., 2018; Potter et al., 2002; Rapp, 2000; Reichert et al., 2009; Sheridan et al., 2000; Yu et al., 2014). The effects of soil organic matter as a cementing agent on rill erodibility mostly depend on the clay percentage and soil water content. Organic matter and clay increase soil structural strength which has been widely documented by several researchers (Amezketa, 1999; Deviren Saygin et al, 2012; 2018; Jastrow, 1996; Puget et al., 2000). Some of fine-textured soils such as the 6th, 7th, 8th, 12th, and 14th soils were good examples of this situation (Tables 1 and 2). Erodibility values were typically lower in soils having greater soil organic matter contents, clay, and MWD values. For example, for the 4th, 6th, 7th, and 9th soils (Fig. 2), changes in the rill erodibilities were notable, depending on the initial moisture conditions.

The relationships between soil properties and erosion resistance are highly dependent on soil texture. In clay-rich soils with low sand content, cohesion and flow properties are critical factors influencing erodibility under saturated conditions. In contrast, sandy soils are more influenced by particle size distribution, which strongly correlates with rill erodibility and critical flow shear stress, particularly under dry and saturated conditions. The unexpected positive correlation between rill erodibility and soil organic matter contents could be related to some potential reasons. Considering that these tested sandy soils have quite high sand contents by weight, the large particles could dominate the soil's behavior, and the addition of organic matter might not be sufficient to overcome the inherent erodibility caused by the lack of fine particles, or the organic matter might be too dispersed to form stable aggregates, especially if the soil is predominantly coarse-textured (Amezketa, 1999; Le Bissonnais, 1996; Nouwakpo et al., 2010).

The most conspicuous point among the findings was the high relationship between the V_f and C_o variables obtained with the cohesion measurement device. This confirms that mechanical cohesion measurements could have the capacity to explain both the particle size distributions and water movement depending on them, as well as to simulate the effects of organic matter and other cementing materials on the structural stability holistically. This supports the view that this approach could have the potential to mechanistically link cohesion estimation to rill erodibility and critical shear stress, and the C_o and V_f variables obtained with this approach can be considered as intrinsic variables in the evaluation of rill initiation in water erosion prediction models (Deviren Saygin et al., 2021; Nouwakpo et al., 2014; Nouwakpo & Huang, 2012).

5. Conclusion

Initial soil moisture content emerges as a pivotal factor influencing rill erosion processes. This study unequivocally demonstrated the impact of soil moisture variations across a diverse spectrum of soil textures, on the rill erodibility parameters K_r and τ_{cr} utilized in the process-based WEPP soil erosion model. Overall findings underscored the complexity of soil behavior and suggest that while moisture content was a key factor in determining rill erodibility and critical flow shear stress, other soil properties could significantly influence this relationship.

Moreover, findings highlighted the promising potential of the mechanical soil cohesion value obtained through the fluidized bed technique. This cohesion parameter emerges as a holistic indicator. The significant correlations obtained between the measured cohesion and the soil erodibility values suggest that cohesion has the potential to explain the complex interactions of various soil properties, particularly their influence on rill erodibility. Cohesion, or the binding force between soil particles, is a critical factor in soil structure and resistance to erosion. Its measurement provides insights into the stability of soil aggregates and how different factors, like organic matter, moisture content, and soil texture, impact the overall erodibility.

This study noted that the WEPP model struggles to predict rill erosion in soils under drainage conditions for small-scale laboratory studies. By incorporating dynamic water table effects and how they interact with soil cohesion in these moisture condition into the WEPP model as an additional parameter, it might improve the model's ability to simulate soil behavior under shallow flow conditions, especially for fine-textured soils. Nonetheless, further comprehensive research is imperative to validate its applicability as a robust model variable across different soil types in forthcoming modeling endeavors.

In essence, the study sheds light on the intricate relationship between soil moisture dynamics, soil properties, and rill erosion processes. By elucidating these relationships, it is expected to contribute to more accurate and comprehensive erosion modeling approaches, essential for effective soil erosion management and conservation strategies in diverse environmental contexts.

Availability of data and materials

The data that support the findings of this study are available from the corresponding author upon reasonable request.

Funding

This study was supported by the Scientific and Technological Research Council of Türkiye (TUBITAK) under Grant Number TUBITAK-3001-118O111. The authors thank TUBITAK for their support.

CRediT authorship contribution statement

Fikret Ari: Writing – review & editing, Writing – original draft, Visualization, Software, Project administration, Methodology, Investigation, Conceptualization. **Selen Deviren Saygin:** Writing – review & editing, Writing – original draft, Visualization, Supervision, Project administration, Methodology, Investigation, Funding acquisition, Formal analysis, Conceptualization. **Cagla Temiz:** Investigation, Data curation. **Sefika Arslan:** Investigation, Data curation. **Mehmet Altay Unal:** Project administration, Conceptualization. **Gunay Erpul:** Writing – review & editing, Writing – original draft, Project administration, Methodology, Conceptualization. **Dennis C. Flanagan:** Writing – review & editing, Writing – original draft, Supervision, Methodology, Conceptualization.

Declaration of competing interest

The authors declare that they have no known competing financial interests or personal relationships that could have appeared to influence the work reported in this paper.

The co-author Dennis C. Flanagan is an Editor-in-Chief for *this journal* (International Soil and Water Conservation Research) and was not involved in the editorial review or the decision to publish this article.

References

Alberts, E. E., Nearing, M. A., Weltz, M. A., Risse, L. M., Pierson, F. B., Zhang, X. C., … Simanton, J. R. (1995). Chapter 7. Soil component. In D. C. Flanagan, & M. A. Nearing (Eds.), *Usda – water erosion prediction Project hillslope profile and watershed model documentation* (pp. 8.1–8.47). USDA-ARS National Soil Erosion Research Laboratory, West Lafayette, Indiana. NSERL Report No. 10.

Amezketa, E. (1999). Soil aggregate stability: A review. *Journal of Sustainable Agriculture, 14*(2–3), 83–151.

Blake, G. R., & Hartge, K. H. (1986). Bulk density and particle density. In *Methods of soil analysis, Part I, physical and mineralogical methods* (2nd ed., pp. 363–381). Madison: ASA and SSSA Agronomy Monograph. no 9.

Bowles, J. E. (1992). *Engineering properties of soil and their measurement* (4th ed., p. 240). New York: McGraw-Hill Book Co.

Brubaker, S. C., Holzhey, C. S., & Brasher, B. R. (1992). Estimating the water-dispersible clay content of soils. *Soil Science Society of America Journal, 56*(4), 1226–1232.

Brunner, A. C., Park, S. J., Ruecker, G. R., Dikau, R., & Vlek, P. L. G. (2004). Catenary soil development influencing erosion susceptibility along a hillslope in Uganda. *Catena, 58*(1), 1–22.

Bryan, R. B. (2000). Soil erodibility and processes of water erosion on hillslope. *Geomorphology, 32*(3–4), 385–415.

Bryan, R. B., & Rockwell, D. L. (1998). Water table control on rill initiation and implications for erosional response. *Geomorphology, 23*(2–4), 151–169.

Caglar, K. O. (1958). *Soil science*. Ankara, Turkey: Ankara University Faculty of Agriculture Publications, No. 10 (In Turkish).

Chenu, C., Le Bissonnais, Y., & Arrouays, D. (2000). Organic matter influence on clay wettability and soil aggregate stability. *Soil Science Society of America Journal, 64*(4), 1479–1486.

Das, B. M. (2008). *Advanced soil mechanics* (3rd ed.). New York: Taylor & Francis Group.

Deviren Saygin, S. (2021). Effects of season and phenology-based changes on soil erodibility and other dynamic RUSLE factors for semi-arid winter wheat fields. *Journal of Agricultural Sciences, 27*(4), 526–535.

Deviren Saygin, S., Arı, F., Temiz, Ç., Arslan, Ş., Ünal, M. A., & Erpul, G. (2021). Analysis of soil cohesion by fluidized bed methodology using integrable differential pressure sensors for a wide range of soil textures. *Computers and Electronics in Agriculture, 191*, Article 106525.

Deviren Saygin, S., Huang, C. H., Flanagan, D. C., & Erpul, G. (2018). Process-based soil erodibility estimation for empirical water erosion models. *Journal of Hydraulic Research, 56*(2), 181–195.

Deviren Saygın, S., Cornelis, W. M., Erpul, G., & Gabriels, D. (2012). Comparison of different aggregate stability approaches for loamy sand soils. *Applied soil ecology, 54*, 1–6.

Ditzler, C., Scheffe, K., & Monger, H. C. (2017). *Soil survey manual. Soil science division Staff*. USDA Handbook 18 (4th ed.). Washington, DC, USA: U.S. Government Printing Office.

Elliot, W. J., Liebenow, A. M., Laflen, J. M., & Kohl, K. D. (1989). *A compendium of soil erodibility data from WEPP cropland field erodibility experiments 1987 and 1988*. West Lafayette, Indiana: The Ohio State University and USDA Agricultural Research Service, National Soil Erosion Research Laboratory. NSERL Report No. 3.

Erpul, G., Gabriels, D., Norton, L. D., Flanagan, D. C., Huang, C. H., & Visser, S. (2013). Raindrop and flow interactions for interrill erosion with wind-driven rain. *Journal of Hydraulic Research, 51*(5), 548–557.

Erpul, G., Şahin, S., İnce, K., Küçümen, A., Akdağ, M. A., Demirtaş, İ., & Çetin, E. (2018). Türkiye su erozyonu atlası. *Çölleşme ve erozyonla mücadele genel müdürlüğü yayınları, Ankara* (In Turkish).

FAO & ITPS. (2015). Status of the world's soil resources (SWSR)—main report. *Food and Agriculture Organization of the United Nations and Intergovernmental Technical Panel on Soils, Rome*, 607.

Flanagan, D. C., Ascough, J. C., Nearing, M. A., & Laflen, J. M. (2001). The water erosion prediction project (WEPP) model. *Landscape erosion and evolution modeling*, 145–199.

Flanagan, D. C., Gilley, J. E., & Franti, T. G. (2007). Water Erosion Prediction Project (WEPP): Development history, model capabilities, and future enhancements. *Transactions of the ASABE, 50*(5), 1603–1612.

Flanagan, D. C., & Livingston, S. J. (Eds.). (1995). *WEPP user summary – water erosion prediction Project* (p. 131). West Lafayette, Indiana: NSERL Report No. 11, National Soil Erosion Research Laboratory, USDA-Agricultural Research Service.

Flanagan, D. C., & Nearing, M. A. (Eds.). (1995). *USDA-Water Erosion Prediction Project: Hillslope profile and watershed model documentation* (p. 289). West Lafayette, Indiana: NSERL Report No. 10, National Soil Erosion Research Laboratory, USDA-Agricultural Research Service.

Flanagan, D. C., & Nearing, M. A. (2000). Sediment particle sorting on hillslope profiles in the WEPP model. *Transactions of the ASAE, 43*(3), 573–583.

Foster, G. R., Flanagan, D. C., Nearing, M. A., Lane, L. J., Risse, L. M., & Finkner, S. C. (1995). Chapter 11. Hillslope erosion component. In D. C. Flanagan, & M. A. Nearing (Eds.), *USDA water erosion prediction Project: Hillslope profile and watershed model documentation* (pp. 11.1–11.12). West Lafayette, Indiana: National Soil Erosion Research Laboratory, USDA-Agricultural Research Service. NSERL Report No. 10.

Govers, G. (1991). Rill erosion on arable land in central Belgium: Rates, controls and predictability. *Catena, 18*(2), 133–155.

Govers, G., Everaert, W., Poesen, J., Rauws, G., De Ploey, J., & Lautridou, J. P. (1990). A long flume study of the dynamic factors affecting the resistance of a loamy soil to concentrated flow erosion. *Earth Surface Processes and Landforms, 15*(4), 313–328.

Grissinger, E. H. (1966). Resistance of selected clay systems to erosion by water. *Water Resources Research, 2*(1), 131–138.

Grissinger, E. H. (1972). Laboratory studies of the erodibility of cohesive materials. *Proceedings Mississippi water resources conference, water resources research institute*. Mississippi, USA: Mississippi State University State College.

Grissinger, E. H., Little, W. C., & Murphey, J. B. (1981). Erodibility of streambank materials of low cohesion. *Transactions of the ASAE, 24*(3), 624–630.

Hanson, G. J., Cook, K. R., & Simon, A. (1999). Determining erosion resistance of cohesive materials. In *American society of civil engineers, international water resources engineering conference*. Seattle, WA, USA.

Huang, C. H., & Laflen, J. M. (1996). Seepage and soil erosion for a clay loam soil. *Soil Science Society of America Journal, 60*(2), 408–416.

Huang, C. H., Laflen, J. M., & Bradford, J. M. (1996). Evaluation of the detachment-transport coupling concept in the WEPP rill erosion equation. *Soil Science Society of America Journal, 60*(3), 734–739.

Jastrow, J. D. (1996). Soil aggregate formation and the accrual of particulate and mineral-associated organic matter. *Soil Biology and Biochemistry, 28*(4–5), 665–676.

Kellogg, C. E. (1993). *Soil survey manual. Soil survey division Staff. USDA handbook* (18, 3rd ed.). Washington, DC, USA: Government Printing Office.

Kemper, W. D., & Rosenau, R. C. (1984). Soil cohesion as affected by time and water-content. *Soil Science Society of American Journal, 48*, 1001–1006.

Kemper, W. D., & Rosenau, R. C. (1986). Aggregate stability and size distribution. In A. Klute (Ed.), *Methods of soil analysis Part 1* (2nd ed., pp. 425–442). Madison, WI: ASA.

Kemper, W. D., Trout, T. J., Brown, M. J., & Rosenau, R. C. (1985). Furrow erosion and water and soil management. *Transactions of the ASAE, 28*(5), 1564–1572.

Klute, A., & Dirksen, C. (1986). Hydraulic conductivity and diffusivity: Laboratory methods. In A. Klute (Ed.) (2nd ed.,*Agronomy monograph No. 9Methods of soil analysis Part 1* (pp. 687–734). Madison, WI: ASA.

Knapen, A., Poesen, J., Govers, G., Gyssels, G., & Nachtergaele, J. (2007). Resistance of soils to concentrated flow erosion: A review. *Earth-Science Reviews, 80*(1–2), 75–109.

Laflen, J. M., Lane, L. J., & Foster, G. R. (1991). Wepp: A new generation of erosion prediction technology. *Journal of Soil and Water Conservation, 46*(1), 34–38.

Le Bissonnais, Y. L. (1996). Aggregate stability and assessment of soil crustability and erodibility: I. Theory and methodology. *European Journal of Soil Science, 47*(4), 425–437.

Lin, F., Chen, X., & Yao, H. (2017). Evaluating the use of Nash-Sutcliffe efficiency coefficient in goodness-of-fit measures for daily runoff simulation with SWAT. *Journal of Hydrologic Engineering, 22*(11), Article 05017023.

Liu, H., Yang, Y., Zhang, K., & Sun, C. (2017). Soil erosion as affected by freeze-thaw regime and initial soil moisture content. *Soil Science Society of America Journal, 81*(3), 459–467.

Mamedov, A. I., Huang, C., & Levy, G. J. (2006). Antecedent moisture content and aging duration effects on seal formation and erosion in smectitic soils. *Soil Science Society of America Journal, 70*(3), 832–848.

McCuen, R. H., Knight, Z., & Cutter, A. G. (2006). Evaluation of the nash–sutcliffe

efficiency index. *Journal of Hydrologic Engineering, 11*(6), 597–602.
Moutier, M., Shainberg, I., & Levy, G. J. (1998). Hydraulic gradient, aging, and water quality effects on hydraulic conductivity of a vertisol. *Soil Science Society of America Journal, 62*(6), 1488–1496.
Nachtergaele, J., & Poesen, J. (2002). Spatial and temporal variations in resistance of loess-derived soils to ephemeral gully erosion. *European Journal of Soil Science, 53*(3), 449–463.
Nash, J. E., & Sutcliffe, J. V. (1970). River flow forecasting through conceptual models part I - A discussion of principles. *Journal of Hydrology, 10*(3), 282–290.
Nearing, M. A., Lane, L. J., Alberts, E. E., & Laflen, J. M. (1990). Prediction technology for soil erosion by water: Status and research needs. *Soil Science Society of America Journal, 54*(6), 1702–1711.
Nearing, M. A., Norton, L. D., Bulgakov, D. A., Larionov, G. A., West, L. T., & Dontsova, K. M. (1997). Hydraulics and erosion in eroding rills. *Water Resources Research, 33*(4), 865–876.
Nelson, D. W., & Sommers, L. E. (1982). Total carbon, organic carbon, and organic matter. In A. L. Page, R. H. Miller, & D. R. Keeney (Eds.), *Method of soil analysis Part 2* (2nd ed., pp. 539–579). Madison, WI: ASA.
Nouwakpo, S. K., & Huang, C. (2012). A fluidized bed technique for estimating soil critical shear stress. *Soil Science Society of America Journal, 76*(4), 1192–1196.
Nouwakpo, S. K., Huang, C., Bowling, L., & Owens, P. (2010). Impact of vertical hydraulic gradient on rill erodibility and critical shear stress. *Soil Science Society of America Journal, 74*(6), 1914–1921.
Nouwakpo, S. K., Huang, C. -h., Weltz, M. A., Pimenta, F., Chagas, I., & Lima, L. (2014). Using fluidized bed and flume experiments to quantify cohesion development from aging and drainage. *Earth Surface Processes and Landforms, 39*(6), 749–757.
Panagos, P., Meusburger, K., Ballabio, C., Borrelli, P., & Alewell, C. (2014). Soil erodibility in europe: A high-resolution dataset based on lucas. *Science of the Total Environment, 479*, 189–200.
Poesen, J. (2007). Recent developments in gully erosion research and their implications for controlling soil loss and sediment yield. In J. Casalí, & R. Giménez (Eds.), *Progress in Gully Erosion Research. IV International Symposium on Gully Erosion. September 17-19, 2007. Pamplona, Spain*. Pamplona: Universidad Pública de Navarra/Nafarroako Unibertsitate Publikoa, 2007. Universidad Pública de Navarra/Nafarroako Unibertsitate Publikoa.
Potter, K. N., Velázquez-Garcia, J. D. J., & Torbert, H. A. (2002). Use of a submerged jet device to determine channel erodibility coefficients of selected soils of Mexico. *Journal of Soil and Water Conservation, 57*(5), 272–277.
Puget, P., Chenu, C., & Balesdent, J. (2000). Dynamics of soil organic matter associated with particle-size fractions of water-stable aggregates. *European Journal of Soil Science, 51*(4), 595–605.
Rapp, I. (2000). *Effects of soil properties and experimental conditions on the rill erodibilities of selected soils* (Doctoral dissertation). Faculty of Biological and Agricultural Sciences. South Africa: University of Pretoria.
Reichert, J. M., Norton, L. D., Favaretto, N., Huang, C., & Blume, E. (2009). Settling velocity, aggregate stability, and interrill erodibility of soils varying in clay mineralogy. *Soil Science Society of America Journal, 73*(4), 1369–1377.
Richards, L. A. (Ed.). (1954). *Diagnosis and improvement of saline and alkali soils (No. 60)*. Washington, DC: US Government Printing Office.
Römkens, M. J., Helming, K., & Prasad, S. N. (2002). Soil erosion under different rainfall intensities, surface roughness, and soil water regimes. *Catena, 46*(2–3), 103–123.
Schieber, J. (2011). Reverse engineering mother nature - shale sedimentology from an experimental perspective. *Sedimentary Geology, 238*(1–2), 1–22.
Shainberg, I., Goldstein, D., & Levy, G. J. (1996). Rill erosion dependence on soil water content, aging, and temperature. *Soil Science Society of America Journal, 60*(3), 916–922.
Shainberg, I., Laflen, J. M., Bradford, J. M., & Norton, L. D. (1994). Hydraulic flow and water quality characteristics in rill erosion. *Soil Science Society of America Journal, 58*(4), 1007–1012.
Shainberg, I., Mamedov, A. I., & Levy, G. J. (2003). Role of wetting rate and rain energy in seal formation and erosion. *Soil Science, 168*(1), 54–62.
Sheridan, G. J., So, H. B., Loch, R. J., & Walker, C. M. (2000). Estimation of erosion model erodibility parameters from media properties. *Soil Research, 38*(2), 265–284.
Simon, A., & Collison, A. J. C. (2001). Pore-water pressure effects on the detachment of cohesive streambeds: Seepage forces and matric suction. *Earth Surface Processes and Landforms, 26*(13), 1421–1442.
Srivastava, A., Wu, J. Q., Elliot, W. J., Brooks, E. S., & Flanagan, D. C. (2017). Modeling streamflow in a snow-dominated forest watershed using the Water Erosion Prediction Project (WEPP) model. *Transactions of the ASABE, 60*(4), 1171–1187.
Tsoar, H. (2005). Sand dunes mobility and stability in relation to climate. *Physica A: Statistical Mechanics and Its Applications, 357*(1), 50–56.
Van Klaveren, R. W., & McCool, D. K. (1998). Erodibility and critical shear of a previously frozen soil. *Transactions of the ASAE, 41*(5), 1315–1321.
Wang, J., Feng, S., Ni, S., Wen, H., Cai, C., & Guo, Z. (2019). Soil detachment by overland flow on hillslopes with permanent gullies in the Granite area of southeast China. *Catena, 183*, Article 104235.
Wang, S., Flanagan, D. C., & Engel, B. A. (2021). Prediction of rill sediment transport capacity under different subsurface hydrologic conditions. *Journal of Hydrology, 598*, Article 126410. https://doi.org/10.1016/j.jhydrol.2021.126410
Wang, S., Flanagan, D. C., Engel, B. A., & McIntosh, M. M. (2021). Impacts of subsurface hydrologic conditions on sediment selectivity and sediment transport in rills. *Catena, 207*, Article 105703. https://doi.org/10.1016/j.catena.2021.105703
Wang, S., Flanagan, D. C., Engel, B. A., & Zhou, N. (2020). Impacts of subsurface hydrologic conditions on rill sediment transport capacity. *Journal of Hydrology, 591*, Article 125582. https://doi.org/10.1016/j.jhydrol.2020.125582
Wang, S., McGehee, R. P., Guo, T., Flanagan, D. C., & Engel, B. A. (2023). Calibration, validation, and evaluation of the Water Erosion Prediction Project (WEPP) model for hillslopes with natural runoff plot data. *International Soil and Water Conservation Research, 11*(4), 669–687.
Wu, Q., Flanagan, D. C., Huang, C., & Wu, F. (2017). Estimation of USLE K-values with a process-based approach. *Transactions of the ASABE, 60*(1), 159–172.
Yu, Y.-C., Zhang, G.-H., Geng, R., & Li, Z.-W. (2014). Temporal variation in soil rill erodibility to concentrated flow detachment under four typical croplands in the Loess plateau of China. *Journal of Soil and Water Conservation, 69*(4), 352–363.
Zhang, X.-C., Li, Z.-B., & Ding, W.-F. (2005). Validation of WEPP sediment feedback relationships using spatially distributed rill erosion data. *Soil Science Society of America Journal, 69*(5), 1440–1447.
Zhang, H. Y., Li, M., Wells, R. R., & Liu, Q. J. (2019). Effect of soil water content on soil detachment capacity for coarse-and fine-grained soils. *Soil Science Society of America Journal, 83*(3), 697–706.
Zheng, F., Huang, C., & Norton, L. D. (2000). Vertical hydraulic gradient and run-on water and sediment effects on erosion processes and sediment regimes. *Soil Science Society of America Journal, 64*(1), 4–11.
Zheng, F., Zhang, X.-C.(J.), Wang, J., & Flanagan, D. C. (2020). Assessing applicability of the WEPP hillslope model to steep landscapes in the northern Loess Plateau of China. *Soil and Tillage Research, 197*, Article 104492.